



FEM-based design for global and local buckling interaction of welded box-section columns

Balázs Kövesdi¹, Mohammad Radwan², László Dunai³

Abstract

Interaction behavior of global (flexural) and local buckling is a widely researched, but currently not solved problem in the design of slender welded box-section columns. In the current recommendations two design methods are available: (i) analytical design approaches, which might consider the coupled stability problem by adjustment of the global or local slenderness ratio of the column, and (ii) finite element method (FEM) based design covering imperfection combinations in the numerical model. Despite numerous previous experimental and numerical results, there is no reliable analytical or FEM-based design approach to determine the buckling resistance. This research topic gets special importance by the increased application of high strength steel structures (yield strength larger than 500 MPa), which might have larger slenderness than columns using normal strength steel increasing the need for the appropriate design for the interacting stability problem. The executed research program investigates the FEM-based design approach emphasizing the imperfections and their combination in the model to achieve appropriate buckling resistance. By the application of equivalent geometric imperfections covering different stability issues the effect of residual stresses will be duplicated leading to conservative buckling resistances. The current paper investigates the imperfection sensitivity of the coupled stability problem and gives design proposal on the imperfection magnitudes to be applied in numerical models for FEM-based design approach.

1. Introduction

Welded box-sections are widely used structural elements for buildings and bridges due to their advantages within the mechanical properties, resistance, easy design, and fabrication processes. The stability behavior of this column type is widely researched, but correctly solved only for the pure flexural buckling and local plate buckling problems. The most conclusive research results for flexural buckling are summarized in the PhD thesis of Somodi (2017) and for local plate buckling in the PhD thesis of Schillo (2017). However, for the typical geometries used in the design praxis the most economic solutions are column geometries, where local (plate) and global (flexural) buckling can also happen, and their interaction should be considered in the design. The

¹ Associate Professor, BME Department of Structural Engineering, Hungary <kovesdi.balazs@emk.bme.hu>

² PhD Student, BME Department of Structural Engineering, Hungary <mohammad.radwan@emk.bme.hu>

³ Professor, BME Department of Structural Engineering, Hungary <dunai.laszlo@emk.bme.hu>

stability issue of these column type gets more attention, especially, if high strength steel structures are used, which are nowadays spreading in the civil engineering praxis. Therefore, the current research focuses on the interaction of local and global buckling resistance of welded box-section columns. Another evolving design method used by civil engineers is the numerical model-based design using direct resistance check, where the ultimate load is determined by geometrical and material nonlinear analysis using imperfections (GMNIA). This design process is currently under significant investigation and ongoing standardization process within Europe. The second-generation Eurocodes is planned to contain a new code part prEN1993-1-14 (2021) summarizing all design rules necessary for the numerical model-based design of steel structures. Within the GMNIA analysis one of the most important parameter is the applied imperfection shape and magnitude. Main part of the previous investigations within this topic were dealing with the imperfections for different structure types and failure modes. However, investigations on the imperfections to be applied for interacting stability problems are missing from the international literature. Therefore, the current research focuses on the imperfections' combinations to be applied to simulate the local and global buckling interaction of welded box-section columns and to determine the interaction buckling resistance using direct resistance check.

The current research program contains a preliminary numerical parametric study focusing on the pure local buckling and pure global buckling, separately. Imperfections to be applied for the welded box-section columns to simulate the flexural buckling and plate buckling are previously determined and presented in recent publications (Radwan et al. 2021) in a detailed manner. The current paper focuses only on the interaction combinations using the preliminary results obtained for pure local and global buckling. Within the GMNIA-based direct resistance check the resistances can be determined using two different design approaches: applying (i) geometric imperfections and residual stresses, or (ii) equivalent geometric imperfections representing the combined effect of geometric imperfections and residual stresses. Reliable equivalent geometric imperfections are determined and proposed for different stability issues in the past. However, if designers are using the combination of the equivalent geometric imperfections and they are adding all possible imperfections related to all possible failure modes (in this case for the local and global buckling), the effect of the residual stresses are duplicated leading to conservative buckling resistances, as observed, and proved by researchers in the past (Degée et al. 2008). Therefore, the investigation of the imperfection combinations to be applied for the interacting stability problems is a key-issue for the accurate buckling resistance calculation. The executed research program contains the followings steps:

- summary of the previous research results on the imperfections for the local and global buckling and standard-based design rules for the imperfection combinations,
- numerical model development and validation on the basis of previous test results,
- determination of accurate interaction buckling resistances using residual stresses and geometric imperfections for the local and global stability issues,
- numerical parametric study to determine the necessary equivalent geometric imperfections and their combinations – within the current study the local plate buckling type imperfection is selected as leading imperfection, further study will investigate the opposite, if global imperfection is taken as leading imperfection,
- determination of the necessary accompanying global equivalent geometric imperfections for different cross-section geometries and column slenderness ratios,
- design model development for the imperfection combinations.

2. Previous investigations and design rules for imperfections

2.1 Previous investigations of interaction buckling

Thus, there is a large number of previous investigations on the local and flexural buckling resistances, there is quite a small number of previous studies on the interaction buckling. Degée et al. (2008) investigated experimentally and numerically the interaction buckling behavior of welded rectangular section columns made of S355 steel grade. Based on the obtained results an upgrade of the European buckling from curve *b* to curve *a* was suggested, as the buckling curve *b* was found too conservative. An enhanced definition of global slenderness ratio was also proposed taking into account the loss of stiffness due to local buckling. Khan et al. (2017) experimentally studied the structural behavior and buckling resistance of slender box-section columns manufactured from HSS. Fifteen specimens are tested and buckling resistances are compared to various international standards. Numerical model was also developed to carry out a numerical parametric study, where $L/1000$ was used as global imperfection and $b/1000$ as local imperfection with accompanying residual stresses. All the numerical and experimental data showed that the results are lying above the buckling curve *b* of the EN 1993-1-1 (2005), which was proposed as the applicable buckling curve determining the interaction buckling resistance.

Yang et al. (2017) investigated numerically and experimentally the interaction buckling behavior of welded box-section columns. Twelve steel columns with medium lengths were tested made of S235 and S355 steel grades. All test specimens failed by interaction buckling mode. Test results showed the current specifications are not taking into account the post-buckling capacity of the plates and therefore, leading to conservative resistances. A numerical parametric study was also performed by Yang et al. (2017) on normal and high strength steel columns. The numerical results show the buckling curve *a* of EN 1993-1-1 (2005) might be applicable instead of the buckling curve *b* for S960 steel grades. It was also noticed that there is a significant influence of residual stresses on the ultimate capacity that can reach up to 20% in the case of medium length columns, which could be considered in an enhanced resistance model.

Further significant research work has been done by Usami and Fukumoto (1982 and 1984), Chiew et al. (1987) and Kwon et al. (2013). The most recent and extensive study has been made by Schillo (2017). She performed thirteen tests on square welded box-section columns with a high b/t ratio made of S500 and S960 steel grades having various global slenderness and performed an extensive numerical parametric study to determine the interaction buckling resistance of the analyzed columns. A unique design approach was developed by Schillo to consider the resistance reduction due to local buckling in the interaction resistance. In this approach, an additional equivalent local geometric imperfection (e_p) was developed to be implemented into the global buckling resistance formula. The proposed equivalent local imperfection can be determined by Eq. (1).

$$e_p = s \cdot \left[\left(\frac{1}{\chi_A} - 1 \right) + \frac{1-\psi}{1+\psi} \cdot \left(\frac{1}{\chi_W} - 1 \right) \right] \quad (1)$$

where: s is equal to the moment of inertia (I) over the area of the section (A) multiplied by the distance from the neutral axis to the maximum fiber (z). The parameters χ_A and χ_W are factors derived using the effective width method $\chi_A = \frac{A_{eff}}{A}$, $\chi_W = \frac{W_{eff}}{W}$, ψ is a modification factor depending on the loading eccentricity. It can be seen that all previous investigations focused on the interaction buckling resistance calculation using analytical design concept applying tabulated

buckling curves validated by experimental and numerical resistance database and statistical evaluation. However, research regarding the FEM-based design approach and proposed imperfections, or imperfections combinations are missing from the international literature.

2.2 Previous investigations of imperfection scaling factors

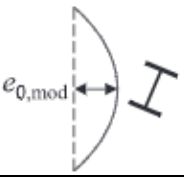
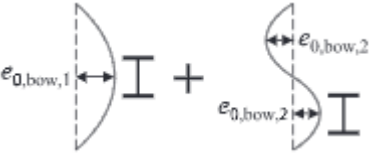
Imperfection scaling factor for member buckling

The most recent research programs in this topic are executed by Walport et al. (2020) investigating the flexural buckling resistance of slender I-section columns and by Quan et al. (2021) investigating the lateral torsional buckling resistance of I-section beams. Both research program had common aims and research strategies executing similar numerical parametric studies leading to design proposal for the applicable imperfection magnitudes separately for flexural and lateral torsional buckling resistances using GMNIA analysis. Important new finding within these research works is that it is realized that the previously developed and standardized equivalent geometric imperfections for member buckling are developed for second order elastic analysis (GNIA) and they are not always applicable within the same form and having the same reliability for geometrically and materially nonlinear (GMNIA) analysis. In both research work, it was shown, that for design by second order elastic analysis (GNIA) following the recommendations of EN1993-1-1 (2005), the magnitudes of the equivalent bow imperfections can be back-calculated to provide the same result as would be obtained from the member buckling curves. However, it was proved, that these equivalent geometric imperfections do not lead to accurate results using GMNIA analysis. Therefore, the equivalent bow imperfections are calibrated against benchmark FE results, generated by GMNIA analysis using imperfections ($L/1000$ geometric imperfection and accompanying residual stresses). Based on the numerical results obtained, an equivalent bow imperfection amplitude according to Eq. (2) is proposed.

$$\frac{e_{0,global}}{L} = \alpha \cdot \beta = \frac{\alpha}{150} \quad \text{but} \quad \frac{e_{0,global}}{L} \geq \frac{1}{1000} \quad (2)$$

where: L is the member length, α is the imperfection factor according to EN 1993-1-1 Table 6.1. The reliability of the proposed approach is evaluated according to EN1990 (2005), and it was shown that partial safety factors of 1.0 for steel and 1.1 for stainless steel can be adopted with accurate safety. Similar back-calculation and numerical parametric study was executed for the lateral torsional buckling resistance calculation by Quan et al. (2021). The aim of the study was to develop equivalent imperfections for use in out-of-plane stability design of steel and stainless steel members by GMNIA. The design proposals are summarized in Table 1.

Table 1: Proposed imperfection magnitudes for lateral torsional buckling

imperfection mode	amplitude
	$e_{0,mod} = \alpha_z \cdot \frac{L}{150} \quad (3)$
	$e_{0,bow,1} = \alpha_z \cdot \frac{L}{150} \quad (4)$
	$e_{0,bow,2} = \alpha_z \cdot \frac{L}{215} \quad (5)$

Two proposals for equivalent imperfection amplitudes are developed: (i) $e_{0,mod}$, for use with eigenmode-affine imperfections; proposal is given by Eq. (3), and (ii) $e_{0,bow}$, for use with sinusoidal hand-defined bow imperfections; proposal is given by Eqs. (4)-(5). The lateral equivalent bow imperfection $e_{0,bow}$ is defined as the summation of a half-sine wave with imperfection amplitude $e_{0,bow,1}$ and a full-sine wave with imperfection amplitude $e_{0,bow,2}$.

Imperfection scaling factor for local buckling

The Winter-type buckling curve provided by the EN 1993-1-5 (2006) has been criticised by many researchers in the past and it has been proved that it is not applicable for welded square box-section columns (Schillo 2017). Therefore, the standardized buckling curve for this specific case was changed and the buckling curve of the Annex B of EN 1993-1-5 is proposed to be used for the buckling resistance calculation. However, if buckling curve is changed, the equivalent geometric imperfection to be applied in FEM-based design processes should be also revised. Therefore, a calibration process was made by Radwan and Kövesdi (2021) for the numerical model based buckling resistance calculation. A numerical parametric study was executed using the same research strategy as applied by Walport et al. (2020) and Quan et al. (2021) for the member buckling cases. The numerical investigations proved that the equivalent geometric imperfection scaling factor to be applied for the plate buckling problems depends on the steel grade (f_y) and the relative slenderness ratio of the analyzed cross-section ($\bar{\lambda}_p$). Two imperfection scaling factors are developed within the parametric study, one for the equivalent geometric imperfections and one for the geometric imperfections to be applied together with residual stresses. The best-fit approximation for the calibrated equivalent geometric imperfection is given by Eq. (6), where $\bar{\lambda}_p$ is the local plate slenderness ratio calculated by Eq. (7), f_y is the nominal yield strength of the analyzed steel material, b is the plate width and σ_{cr} is the critical plate buckling stress under pure compression.

$$\frac{b}{e_{0,local}} = \left\{ \begin{array}{ll} \frac{1}{\bar{\lambda}_p^{2.2}} \cdot (200 - 0.2 \cdot f_y) & \text{if } \bar{\lambda}_p \leq 1.35 \\ \frac{1}{\bar{\lambda}_p} \cdot (160 - 0.2 \cdot f_y) & \text{if } \bar{\lambda}_p > 1.35 \end{array} \right\} \quad (6)$$

$$\bar{\lambda}_p = \sqrt{\frac{f_y}{\sigma_{cr}}} \quad (7)$$

Based on the executed numerical parametric study it was proved that the application of this equivalent geometric imperfections leads to buckling resistances showing very good agreement to the currently best plate buckling curve developed by Schillo (2017) and the resistances are close to the buckling resistances provided by the Annex B buckling curve of the EN 1993-1-5 (2006).

2.3 Design proposal of the new prEN 1993-1-14 (2021)

A new code prEN 1993-1-14 (2021) is currently under development in Europe which will provide design rules to FEM-based design of steel structures. This code also contains the imperfections to be applied. According to these design rules, imperfections should account for the effects of geometric deviations from the perfect shape, residual stresses and boundary

condition defects (e.g. uneven foundation, etc.). One of the following imperfection types may be applied in the numerical model:

- a. geometric imperfections and additional residual stresses due to fabrication,
- b. equivalent geometric imperfections by modification of the perfect shape of the structure; these imperfections are intended to cover the effect of both the geometrical imperfections and the residual stresses and have larger magnitudes than solely geometric imperfections.

Concerning to plated structures the prEN 1993-1-14 classifies the equivalent geometric imperfections into three sub-groups which are the bases of the imperfection combinations:

- equivalent geometric imperfections for global structures (e.g. frames),
- equivalent geometric imperfections for structural members (e.g. beam/column),
- equivalent geometric imperfections for cross-sections (e.g. plates).

For the member type imperfections, the latest research results introduced in Section 2.2 are considered within the code. For the plate buckling type imperfections the proposal for the EN 1993-1-5 (2006) Annex C are considered without any changes. Regarding the imperfection combinations, the following simple rules are introduced. Where both geometric imperfections and residual stresses are used, all the geometric imperfections and the residual stresses should be applied to the model at the same time, with their nominal values. Where equivalent geometric imperfections arising from different sub-groups are being used (e.g. frame, member and cross-sectional imperfections) each imperfection should be taken with its maximum amplitude and they should be linearly added. For equivalent cross-section imperfections in plated structures, the combination of the imperfections might be necessary. The leading imperfection should be chosen first, with accompanying imperfections at amplitudes reduced to 70% of the defined value. Each imperfection type in turn should be chosen as the leading imperfection, with the remainder taken as the accompanying imperfections (prEN1993-1-14, 2021).

3. Numerical modeling

3.1 Numerical model development

A parametric numerical model is developed using FE program ANSYS 18.5 using four-node thin shell elements. The general layout of the numerical model is shown in Fig. 1, presenting the geometrical model of the box-section columns with finite element mesh and imperfections. Within the current analysis only square box-section columns are analyzed, which are always double symmetric. The applied imperfections related to local, global and interaction buckling are separately presented in Fig. 1. For local imperfections (Fig. 1a) half-sine waves are applied at each panel of the cross-section having alternating direction. The global imperfection is a half-sine wave along the entire column length (Fig. 1b) representing the buckling length of the analyzed columns. To determine the interaction buckling resistance the local and global imperfections are combined, as shown in Fig. 1c. The magnitudes of the applied imperfections are detailed later in Sections 4 and 5. In the current analysis, hand-defined half-sine wave shapes are used as imperfections, but the numerical analysis also proved the given imperfection magnitudes are also applicable by using the first eigenmode shape as imperfections. Two master nodes are defined in the center of gravity of the end cross-sections. Rigid diaphragms were used to link all the 6 DOFs between the master nodes and all the nodes at the end cross-sections using rigid members. The movement of one of the master nodes is restricted against translation in (UX,

UY, UZ) global directions and restrained against rotation along the longitudinal axis (RZ), while the other master node is allowed to move in the UZ direction allowing to apply the compression force on the column.

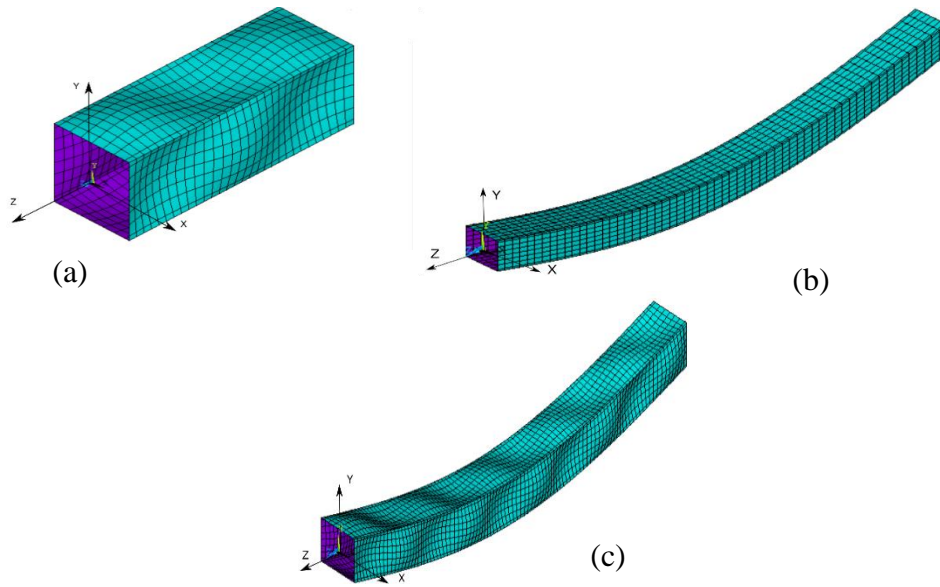


Figure 1: a) Local, b) global, and c) interaction definitions of imperfections

The applied material model presented in Fig. 2 is an elastic-plastic quad-linear material model proposed by Gardner et al. (2019) for NSS grades and introduced in prEN1993-1-14. The material models behave linearly elastic up to the yield strength (f_y) by obeying the Hooke's law with Young's modulus (E) equal to 210000 MPa. The yield plateau is modelled between ϵ_y and ϵ_{sh} and an isotropic hardening behavior is modelled until reaching the ultimate strength ($f_u; \epsilon_u$). In the current analysis S355 steel grade is used having nominal values for the yield and ultimate strengths ($f_y=355$ MPa, $f_u=510$ MPa), respectively. The parameters of the material model are given in Table 2.

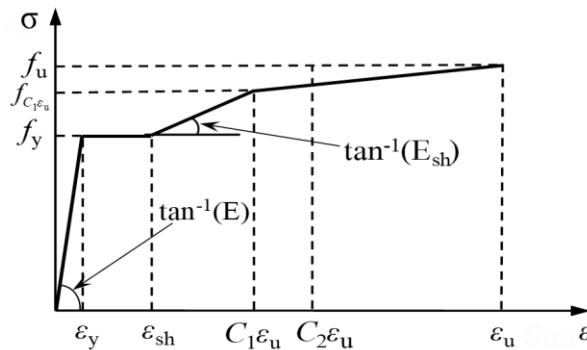
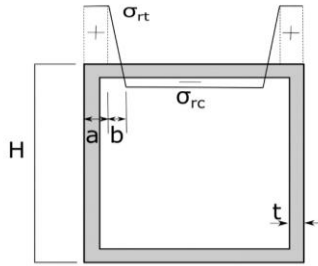


Figure 2: Applied material model according to prEN 1993-1-14

Table 2: Parameters of the applied material model

	f_y [MPa]	f_u [MPa]	ϵ_{sh}	ϵ_u	C_1	C_2	E_{sh} [MPa]	$C_1 \cdot \epsilon_u$	$f_{C1\epsilon_u}$
S355	355	510	0.015	0.182	0.310	0.448	2310	0.057	451

A well-established, standardized residual stress pattern is applied in the numerical model according to the recommendations of the ECCS (European Convention for Constructional Steelworks, 1988) and prEN1993-1-14 (2021). The details of this model are given in Fig. 3. The tensile stress is always taken equal to the yield strength. The compressive residual stress is taken according to Fig. 3 and based on the equilibrium of the tensile and compressive stresses. Parameters a and b define the distance of each plate subjected to tensile stresses near each corner of the section. The H/t ratio for the vast majority of the cross-section within the current study is larger than 40 to study class 4 (slender) sections, which are sensitive for local buckling.



H/t	Welding type	σ_{rt}/f_y	σ_{rc}/f_y	a	b
10	–	1.0	-0.60	0	–
20	Heavy weld	1.0	-0.82	$3t$	$3t$
20	Light weld	1.0	-0.29	$1.5t$	$1.5t$
40	Heavy weld	1.0	-0.29	$3t$	$3t$
40	Light weld	1.0	-0.13	$1.5t$	$1.5t$

Figure 3: Parameters of the residual stress model

3.2 Model validation and verification

At first a mesh sensitivity analysis is performed to obtain an appropriate mesh size yielding to accurate results in a reasonable time to verify the numerical model. The mesh sensitivity study is performed for the smallest and the largest plate width within the parametric study and it was shown that 16 elements along the plate widths ensures an FE mesh which is fine enough to obtain accurate buckling resistance. For all other cases the applied element number has been regulated to keep the same width-to-element number ratio. As a second step the numerical model is validated by comparison of the computed load-deformation curve and ultimate load to test results. In the entire research program, a total of 15 test specimens taken from four different experimental research programs are selected and used for the model validation. Two samples from 15 cases are shown in Figs. 4-5 to demonstrate the accuracy of the numerical model.

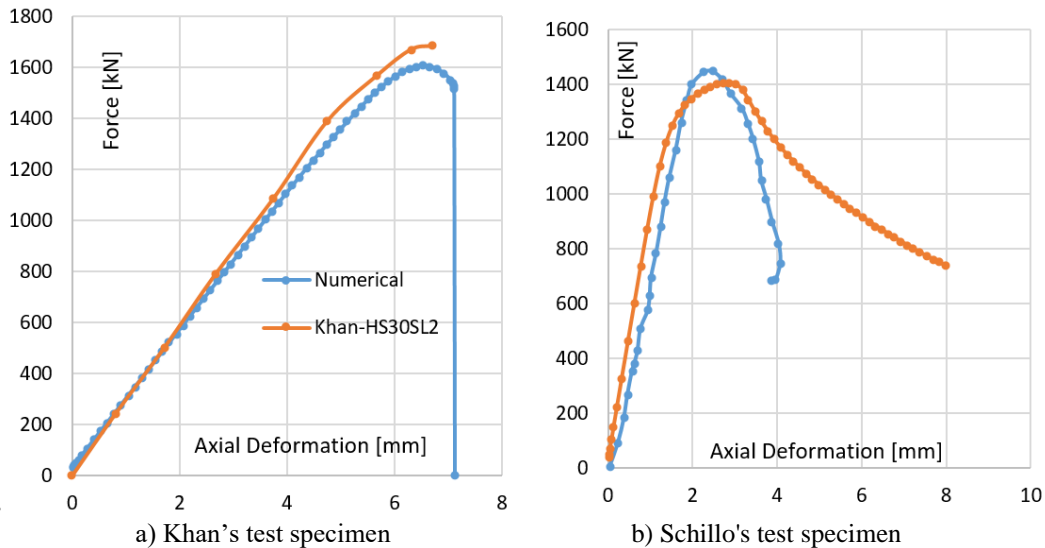


Figure 4: Comparison of measured and computed load-deformation curves

The figure on the left shows a test result taken from the research program of Khan et al. (2016) and on the right-hand side is taken from Schillo (2017). Both comparisons show a very good agreement between the numerical and the experimental results demonstrating that the developed numerical model is capable to follow the interaction buckling phenomena and provides accurate buckling resistance. The failure mode and the obtained deformation and stress distribution is shown in Fig. 5 for one test specimen to demonstrate the obtained failure modes.

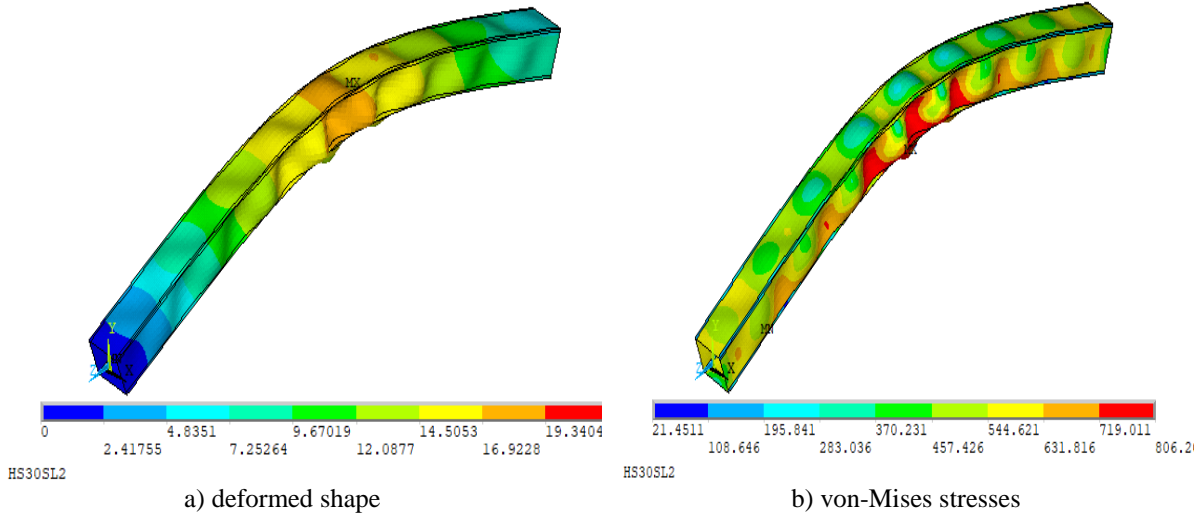


Figure 5: Obtained failure mode for interaction buckling at the final step of loading of Khan's test specimen

3.3 Investigated parameter range

The executed numerical parametric study aims to create a large database to study the interaction buckling resistance and imperfection sensitivity of columns having different local and global slenderness ratio. Therefore, the b/t ratio of the analyzed cross-sections and the columns length are varied within a wide parameter range. The applied geometries, combination of $b=h$ and t values are listed in Table 3. More than 2000 GMNI analyses are performed investigating 50 different cross-sections and 15 column lengths for each. The local slenderness ratio is varied between 0.7 to 2.8, while the global slenderness ratio is changed between 0.2 and 2.6. For each column geometry many analyses are executed using different imperfection combinations, as presented in the following sections.

Table 3: Geometrical properties of the analysed cross-sections

	$b = h$ [mm]	thickness values [mm]	lengths [mm]
1	200	2.0; 2.5; 3.0; 3.5; 4.0; 4.5; 5.0; 5.5; 6.0; 6.5	750; 1750; 2500; 3000; 3750; 5000; 6250; 7500; 8750; 10000; 11250; 12500; 15000; 17500; 20000
2	250	2.0; 2.25; 2.5; 2.75; 3.0; 3.25; 3.5; 4.0; 5.0; 6.0; 7.0; 8.0	
3	350	2.75; 3.0; 3.5; 4.0; 4.5; 5.0; 5.5; 6.0; 6.5; 7.0; 8.0; 9.0; 10.0	
4	450	3.75; 4.0; 4.25; 4.5; 4.75; 5.0; 5.25; 5.5; 5.75; 6.0; 6.5; 7.0; 8.0; 9.0; 10.0	

4. Analysis of imperfection combinations

4.1 Applied imperfections and combinations

In the applied numerical parametric study at first the buckling resistances are determined using different imperfection combinations and results are compared and evaluated. The applied imperfection combinations investigated in the current study are summarized in Table 4. At first, buckling resistances are determined using combination of residual stresses and geometric imperfections, which calculation is considered as leading to the most accurate buckling resistance for this column-type and cited as “accurate resistance” in the followings. For box-section columns there are many different residual stress patterns proposed in the international literature; within the current study the most reliable, well-established, test-based residual stress pattern recommended by ECCS (1988) is applied, which is also implemented into the new prEN 1993-1-14 (2021). The geometric imperfection for the global buckling is taken by $L/1000$, which is also an accepted value to determine the flexural buckling resistance. These imperfections serve as background for the Eurocode-based flexural buckling curves. For the local buckling imperfections, the previously proposed and calibrated imperfection scaling factor ($b/f_{local,geom}$) is applied, developed by Radwan and Kövesdi (2021). This imperfection scaling factor leads to plate buckling resistances following the most accurate buckling curve developed by Schillo (2017). The proposed buckling curve of Schillo is calibrated to many test results using statistical evaluation and numerical simulation results made on normal and high strength steel box-section columns. The buckling resistance determined using the combination of the above given residual stresses and geometric imperfections are considered as the most accurate buckling resistance for the local and global buckling interaction serving as target values for the further investigations.

Table 4: Applied imperfection combinations

	global imperfection	local imperfection	residual stresses
Accurate resistance	$L/1000$ according to Eurocode-based buckling curve development processes	$b / f_{local,geom}$ proposed geometric imperfections by Radwan and Kövesdi (2021) representing buckling curve developed by Schillo (2017)	ECCS residual stress patterns
Imp. combination #1	$L/200$ according to EN 1993-1-1 – buckling curve b	$b / 200$ according to EN 1993-1-5 and EN 1993-1-14	-
Imp. combination #2	$\alpha \cdot L/150$ according to EN 1993-1-14 – $\alpha = 0.34$	$b / 200$ according to EN 1993-1-5 and EN 1993-1-14	-
Imp. combination #3	$\alpha \cdot L/150$ according to EN 1993-1-14 – $\alpha = 0.34$	b / f_{local} proposed equivalent geometric imperfection by Radwan and Kövesdi representing buckling curve developed by Schillo (2017)	-

After determining the most accurate buckling resistance three different imperfection combinations are analyzed, and the buckling resistances are compared. In the case of imperfection combination #1, global imperfection with amplitude of $L/200$ is applied, which is the current proposal of the EN 1993-1-1 (2005) for plastic analysis representing buckling curve b . For the local imperfection $b/200$ is used as equivalent geometric imperfection magnitude which is proposed by prEN 1993-1-14 (2021) taken from EN 1993-1-5 (2006) Annex C. In the

case of imperfection combination #2 the global imperfection is changed according to the most recent research results of Walport et al. (2020) proposing buckling curve dependent imperfection scaling factor. The new scaling factor is implemented into the prEN 1993-1-4, and it was combined with the $b/200$ local imperfection. As a third option (imperfection combination #3) the local imperfection is also changed according to the most recent improvement of Radwan and Kövesdi (2021). The proposed equivalent geometric imperfection is developed for box-section columns and calibrated to the currently most accurate buckling curve developed by Schillo (2017). The imperfection scaling factor according to this proposal depends on the local slenderness ratio ($\bar{\lambda}_p$) of the analyzed cross-section and the yield strength (f_y) of the steel material. The best-fit approximation of the calibrated scaling factor is given by Eq. (8).

$$f_{local} = \begin{cases} \frac{1}{\bar{\lambda}_p^{2.2}} \cdot (200 - 0.2 \cdot f_y) & \text{if } \bar{\lambda}_p \leq 1.35 \\ \frac{1}{\bar{\lambda}_p} \cdot (160 - 0.2 \cdot f_y) & \text{if } \bar{\lambda}_p > 1.35 \end{cases} \quad (8)$$

4.2 Comparison of buckling resistances

For all analyzed columns the buckling resistances are determined using these three different imperfection combinations summarized in Table 4. At first the buckling resistance are compared to each other and presented in Fig. 6. The vertical axis represents the buckling resistance according to the accurate solution and the horizontal axis the buckling resistance using the three different imperfection combinations. It can be seen from the results that load case combination #1 has the largest scatter and there are results on the safe and unsafe side as well. Load case combination #3 is the only providing solutions always on the safe side in the entire analyzed parameter range. Similar comparisons showing the results depending on the local or global slenderness are given in Figs. 7-10 making possible to evaluate the results more in details. The vertical axis of these graphs represents the ratio of the accurate and the computed resistance using different imperfection combinations; the horizontal axis shows the slenderness ratio.

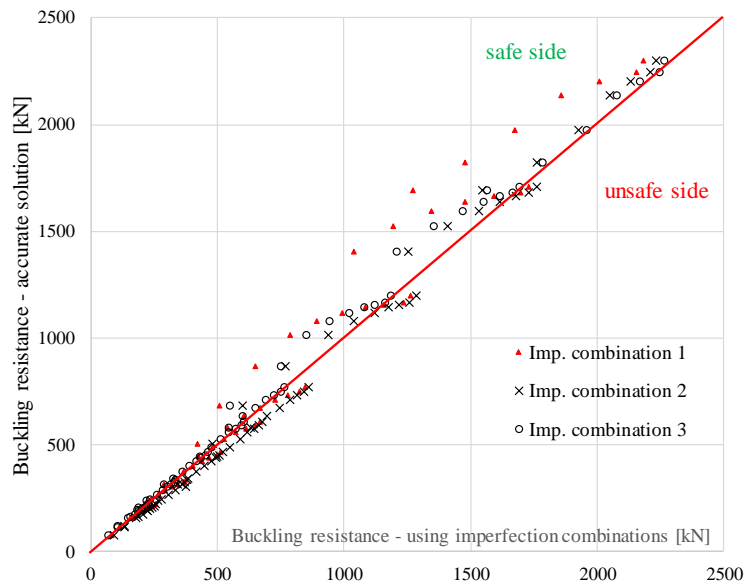


Figure 6: Comparison of the accurate resistances to buckling resistances using different imperfection combinations

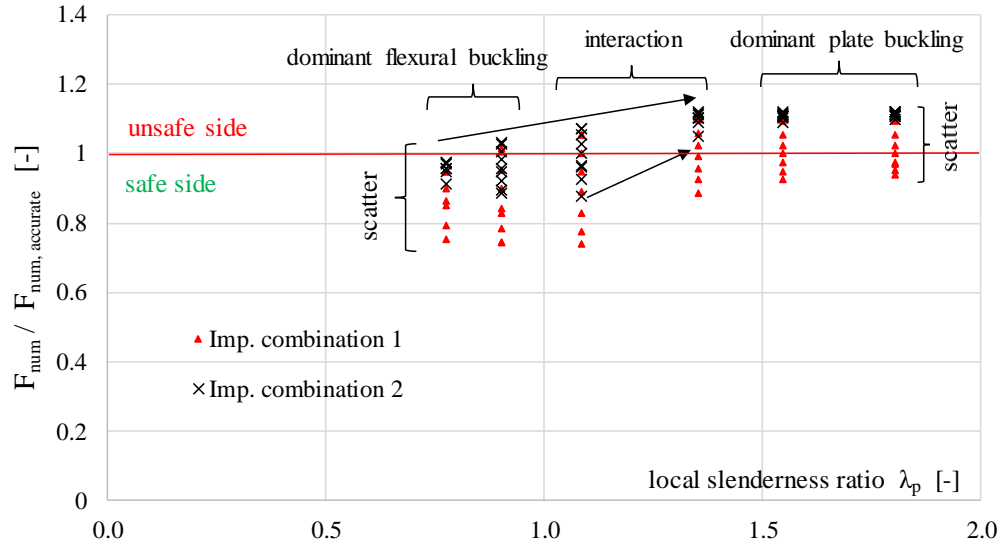


Figure 7: Comparison of buckling resistances – relationship with local slenderness ratio – 1

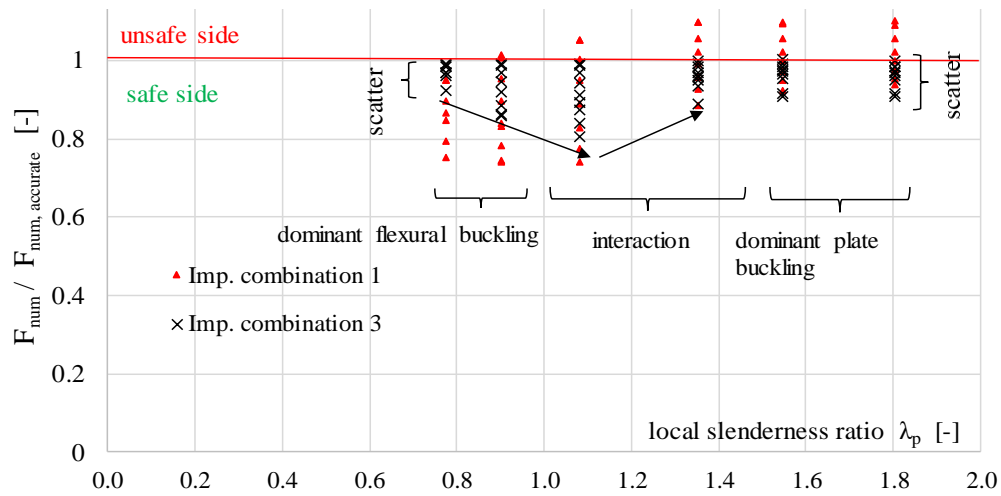


Figure 8: Comparison of buckling resistances – relationship with local slenderness ratio – 2

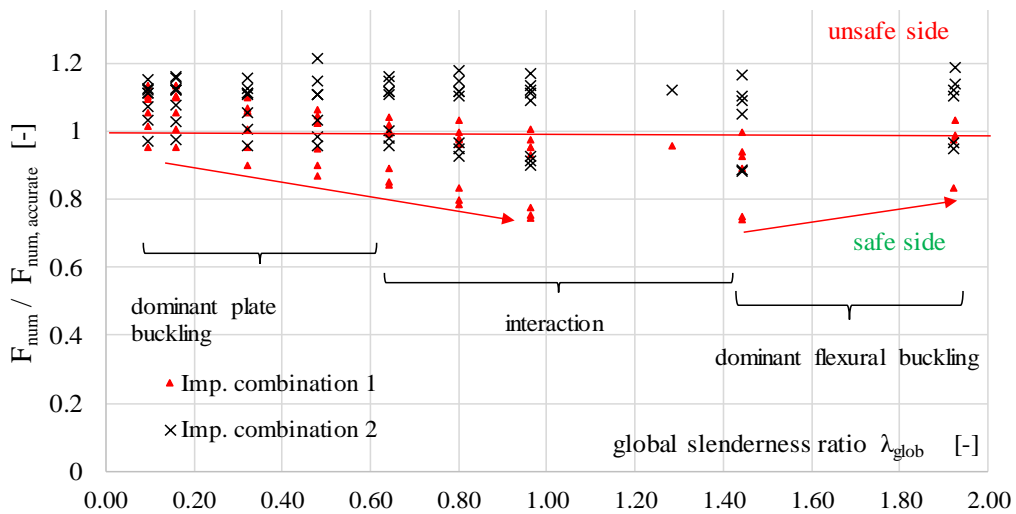


Figure 9: Comparison of buckling resistances – relationship with global slenderness ratio – 1

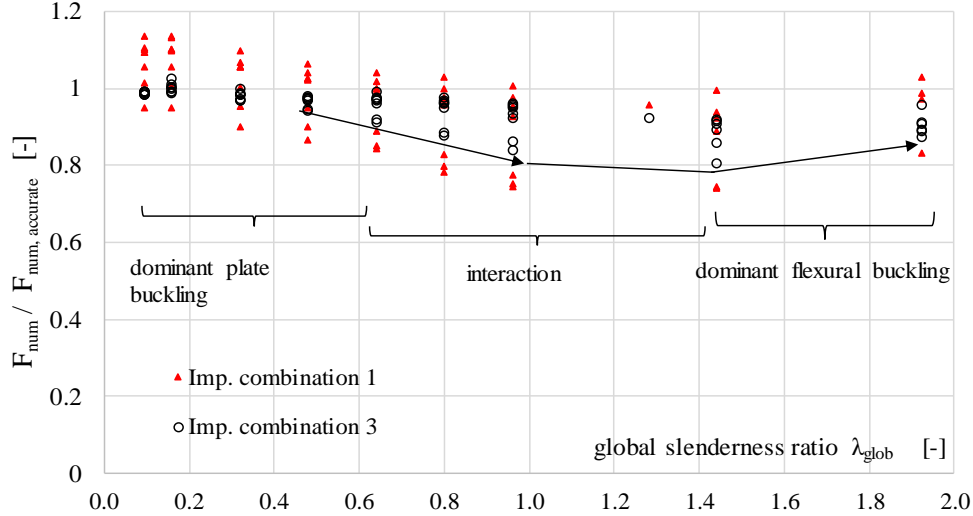


Figure 10: Comparison of buckling resistances – relationship with global slenderness ratio – 2

Results show different imperfection combinations has different impact on the buckling resistance depending on the global and local slenderness ratio. Therefore, the results are separately evaluated depending on the $\bar{\lambda}_p$ and $\bar{\lambda}_{glob}$ slenderness ratios. Results show the buckling resistances using the imperfection combination #1 gives the largest scatter quasi-uniform within the entire local slenderness region. However, buckling resistances within the small slenderness range are mainly on the safe side, for the large local slenderness range on the unsafe side. Similar trends can be obtained for the resistances using the load case combination #2 but having significantly smaller scatter. Only the imperfection combination #3 can ensure, that the buckling resistances for the interacting buckling phenomena are in the entire analyzed parameter range on the safe side. However, results prove for the interaction domain the scatter is significantly larger (shown in Fig. 8 by the black arrows) than in case of pure flexural buckling or local plate, for which the imperfection magnitudes are calibrated. Similar trends are shown in Figs. 9-10, presenting all the results depending on the global slenderness ratio. Results prove application of imperfection combination #1 leads to safe or unsafe side resistance depending on the slenderness ratio. The application of the improved global buckling imperfection scaling factor corrects this trend (imperfection combination #2) and provides uniform scatter along the entire global slenderness range. The application of the local imperfection scaling factor proposed by Radwan and Kövesdi (2021) pushes all results to the safe side, meaning that both modifications are necessary. However, the scatter significantly increases in the interaction domain proving the importance of the imperfection combination rules. The comparison of the buckling resistances and the statistical evaluation of the numerical calculations are summarized in Table 5 presenting the minimum, maximum and the average values and the standard deviations for the obtained resistance ratios.

Table 5: Comparison of buckling resistances using different imperfection combinations

	Imp. combination 1	Imp. combination 2	Imp. combination 3
Min.	0.741	0.879	0.806
Max.	1.135	1.213	1.024
Average	0.974	1.070	0.953
Cov.	0.107	0.079	0.047

These results prove the proposal of Walport et al. (2020) works well for flexural buckling and makes the scattering significantly smaller for dominant flexural buckling. The proposal of Radwan and Kövesdi (2021) works well for dominant local buckling and makes all the computed resistances on the safe side. However, in the interaction buckling domain the scatter of the results is quite large proving that the imperfection combinations need improvement, thus the application of both the global and local imperfection magnitudes can lead to conservative results.

5. Imperfection combination proposal development

After the analysis of the buckling resistances using different imperfection combinations the accurate imperfection magnitudes are also determined which could be used in imperfection combinations. The proposed strategy of the prEN 1993-1-4 is applied, thus one leading imperfection is selected and the necessary magnitude for the accompanying imperfections is determined. Within the current study the local plate buckling type imperfection is selected as leading imperfection (considered always with 100% power) and a numerical parametric study is executed to determine how large should be the global member-type imperfection to reach the accurate buckling resistance. One example for the imperfection sensitivity study is presented in Fig. 11. In the figure the vertical axis represents the buckling resistance, the orange vertical line represents the accurate solution, and the blue points represent the numerical calculations results with 100% local imperfection and accompanying global imperfection (according to Eq. (9)). By the intersection point of the two lines, the necessary imperfection magnitude of the global imperfection is determined for all analyzed column geometries.

$$e_0 = 100\% \cdot e_{local} + x\% \cdot e_{0,global} \quad (9)$$

where $e_{0,local}$ is defined by Eq. (8) and $x\% e_{0,local}$ is the value to be determined. The imperfection scaling factor is considered as the buckling length divided by the imperfection scaling factor (L/f_{global}). The value of f_{global} is presented on the horizontal axis of Fig. 11.

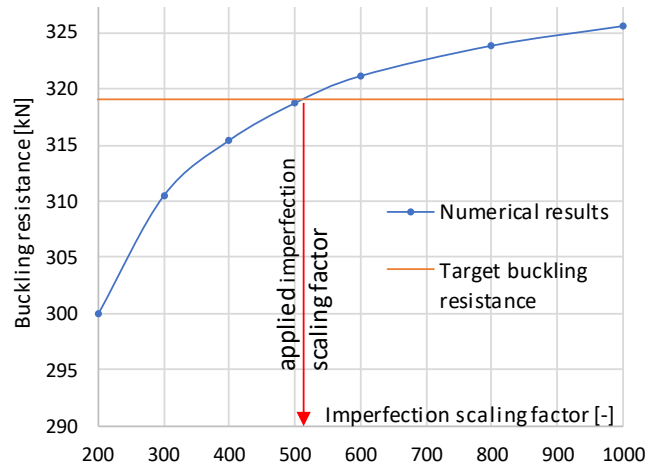


Figure 11: Results of imperfection sensitivity study and determination of necessary imperfection scaling factor for the accompanying global imperfection

The necessary imperfection scaling factors are determined for all analyzed column geometries and the determined scaling factors are evaluated in the function of the global ($\bar{\lambda}_{glob}$) and local

($\bar{\lambda}_p$) slenderness ratios. The obtained results are presented in Fig. 12; the vertical axis represents the determined imperfection scaling factor, and the horizontal axis shows the global slenderness ratio. The five diagrams represent columns having five different local slenderness ratios.

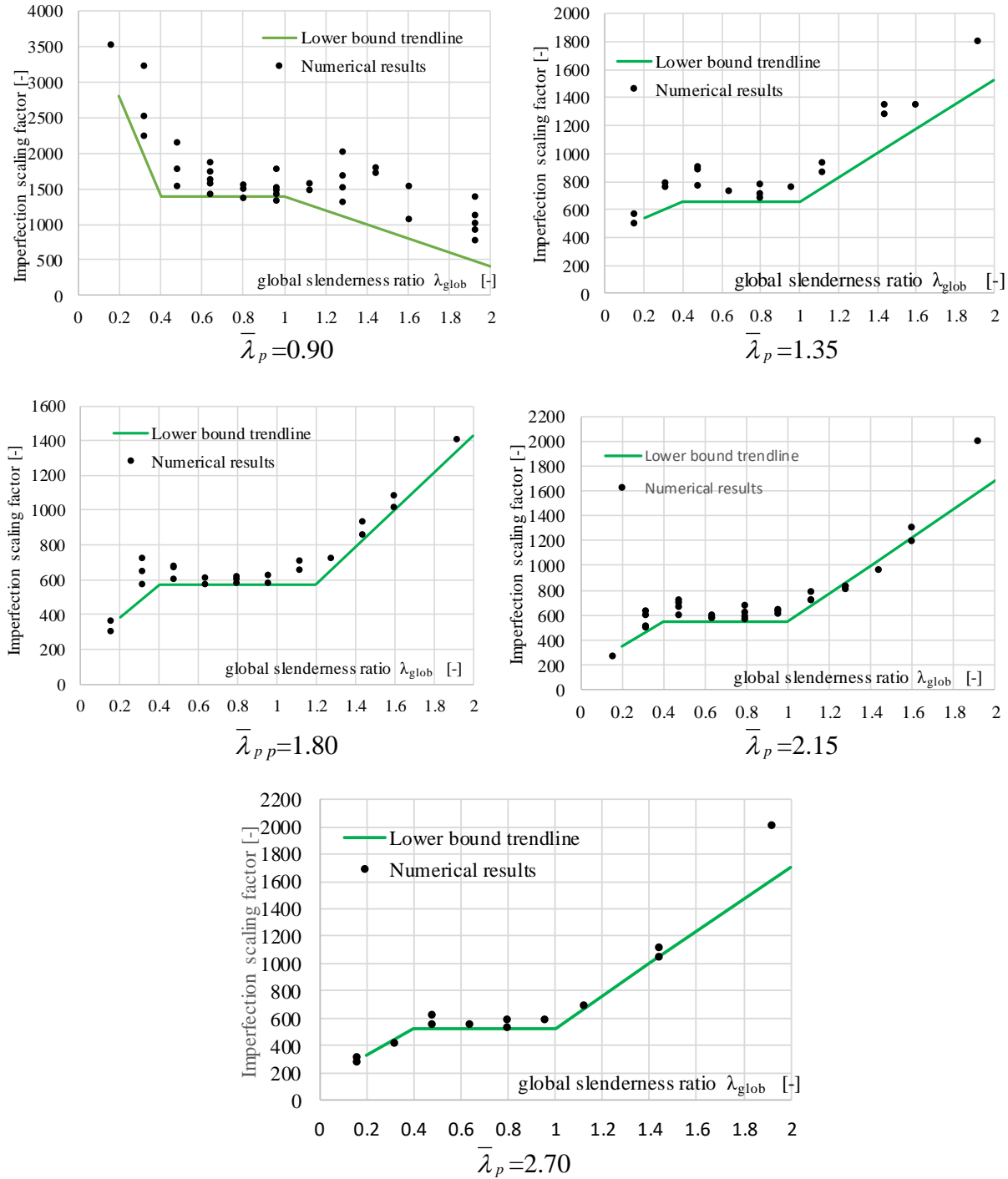


Figure 12: Numerical results and obtain trendlines for the accompanying global imperfections

Results show there is a clear trend in the necessary accompanying global equivalent geometric imperfections which can be characterized by the global and local slenderness ratios. The

diagrams also contain lower bound trendlines showing the obtained trends for the necessary imperfections. The physical meanings and explanations of the obtained results are the followings:

- the accompanying equivalent geometric imperfection should be larger than $L/1000$ (global geometric imperfection) for many different slenderness values, meaning that the effect of the residual stresses for flexural buckling are not covered by the leading local equivalent geometric imperfection alone,
- the proposed equivalent geometric imperfection $\alpha \cdot L/150$ gives minimum values for the obtained accompanying imperfections, meaning that the imperfection can be significantly reduced, if imperfection combinations are applied,
- at the main interaction domain (moderate local and global slenderness) the accompanying global imperfection is between $L/500 - L/1400$ depending on the local slenderness ratio,
- if both the global and local slenderness ratios are large, the accompanying imperfection can be significantly smaller than its basic value ($\alpha \cdot L/150$),
- if both the global and local slenderness ratios are small, the accompanying imperfection can be significantly smaller than its basic value ($\alpha \cdot L/150$),
- in the interaction domain there is a smooth transition characterized by the presented trendlines in Fig. 12.

It can be seen all the trendlines have similar character and the corner points are located at similar global slenderness ratios. Therefore, a model is created presented in Fig. 13 giving the necessary imperfection scaling factor (f_{global}) in the function of the global ($\bar{\lambda}_{glob}$) and local ($\bar{\lambda}_p$) slenderness ratios. The obtained imperfections have clear physical background and gives the necessary imperfection magnitudes depending on the slenderness ratio alone. The values of the vertical axis are given by Eqs. (10)-(12) making the adjustment to the trendlines presented in Fig. 12.

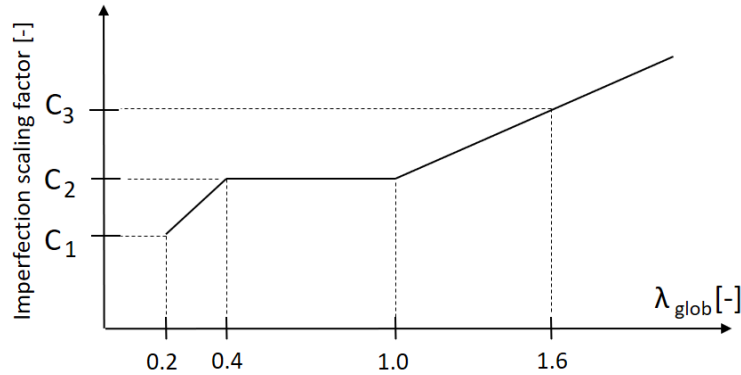


Figure 13: Proposed model for accompanying global geometric imperfections

$$C_1 = 300 + \frac{100}{(\lambda_p - 0.7)^2} \quad (10)$$

$$C_2 = 500 + \frac{80}{(\lambda_p - 0.7)^{1.5}} \quad (11)$$

$$C_3 = 1000 \quad (12)$$

6. Conclusions

Numerical research program is executed to investigate the effect the imperfection combinations on the local and global buckling interaction of welded box-section columns. Based on the numerical simulation results the following conclusions are drawn:

- the applied imperfection combination has significant influence on the obtained buckling resistance, which can reach up to $\pm 25\%$ difference compared to accurate resistance,
- the imperfection proposal of Walport et al. (2020) applied in prEN 1993-1-14 (2021) for the global imperfection gives accurate results for dominant global buckling cases,
- the imperfection proposal of Radwan and Kövesdi (2021) for the local imperfection gives accurate results for dominant plate buckling cases,
- for the interaction domain the combination of these two imperfections (acc. to Walport et al. and Radwan and Kövesdi) provides always safe side resistances,
- however, for most accurate resistance prediction an imperfection combination rule is developed and presented in the current paper taking always the local buckling type imperfection as leading imperfection and the global buckling type imperfection as accompanying one.

Further investigations are planned within this topic to investigate the necessary imperfection combination for the case if global imperfection is taken as leading imperfection and the local imperfection would be the accompanying one. Within the design process both imperfection combinations could be used leading to accurate buckling resistance.

Acknowledgments

The presented research program is financially supported by the Grant MTA-BME Lendület LP2021-06 / 2021 “Theory of new generation steel bridges” program of the Hungarian Academy of Sciences and Stipendium Hungaricum Scholarship. Both grants are gratefully acknowledged.

References

- ANSYS® v16.5, Canonsburg, Pennsylvania, USA.
- Chiew, S.P., Lee, S.L., Shanmugam, N.E. (1987) “Experimental study of thin-walled steel box columns,” *Journal of Structural Engineering*, 113 (10), 2208-2220.
- Degée, H., Detzel, A., Kuhlmann, U. (2008) “Interaction of global and local buckling in welded RHS compression members,” *Journal of Constructional Steel Research*, 64 (7), 755-765. doi: 10.1016/j.jcsr.2008.01.032.
- ECCS (1988) “European recommendations for steel construction; buckling of steel shells”.
- EN 1990 (2005) Eurocode 0: Basis of structural design, European Committee for Standardization (CEN).
- EN 1993-1-1 (2005) Eurocode 3: Design of steel structures, Part 1-1: General rules and rules for buildings.
- EN 1993-1-5 (2006) Eurocode 3: Design of steel structures, Part 1-5: Plated structural elements.
- Gardner, L., Yun, X., Fieber, A., Macorini L. (2019) “Steel design by advanced analysis: material modeling and strain limits,” *Engineering*, 5 (2), 243-249. doi: <https://doi.org/10.1016/j.eng.2018.11.026>.
- Khan, M., Uy, B., Tao, Z., Mashiri, F. (2016) “Concentrically loaded slender square hollow and composite columns incorporating high strength properties,” *Engineering Structures*, 131, 69-89. doi: <https://doi.org/10.1016/j.engstruct.2016.10.015>.
- Kwon, Y.B., Seo, E.G. (2013) “Prediction of the compressive strength of welded RHS columns undergoing buckling interaction,” *Thin-Walled Structures*, 68, 141-155. doi: 10.1016/j.tws.2013.03.009.
- prEN 1993-1-14 (2021) Eurocode 3: Design of steel structures, Part 1-14: Design assisted by finite element analysis (under development).
- Quan, Ch., Walport, F., Gardner, L. (2021) “Equivalent imperfections for the out-of-plane stability design of steel beams by second-order inelastic analysis,” *Engineering Structures*, 251, 113481. doi: 10.1016/j.engstruct.2021.113481

- Radwan, M., Kövesdi, B. (2021) "Local plate buckling type imperfections for NSS and HSS welded box-section columns," *Structures*, 34, 2628-2643. doi: 10.1016/j.istruc.2021.09.011.
- Schillo, N. (2017) "Local and global buckling of box columns made of high strength steel," PhD thesis, RWTH Aachen.
- Schillo, N., Feldmann, M. (2018) "Interaction of local and global buckling of box sections made of high strength steel", *Thin-Walled Structures*, 128, 126-140. doi: <https://doi.org/10.1016/j.tws.2017.07.009>.
- Somodi, B. (2017) "Flexural buckling resistance of high strength steel welded and cold-formed square closed section columns," PhD thesis, Budapest University of technology and Economics.
- Usami, T., Fukumoto, Y. (1983) "Local and overall buckling of welded box columns," *J. Struct. Div.*, 108 (3), 525-542.
- Usami, T., Fukumoto, Y. (1984) "Welded box compression members," *Journal of Structural Engineering*, 110 (10), 2457-2470.
- Walport, F., Gardner, L., Nethercot, D.A. (2020) "Equivalent bow imperfections for use in design by second order inelastic analysis," *Structures*, 26, 670-685. doi: 10.1016/j.istruc.2020.03.065.
- Yang, L., Shi, G., Zhao, M., Zhou, W. (2017) "Research on interactive buckling behavior of welded steel box-section columns," *Thin-Walled Structures*, 115, 34-47. doi: <https://doi.org/10.1016/j.tws.2017.01.030>.